



## Analysis of thermophysical properties of CuO nanoparticles in Water and Ethylene Glycol Based Fluids

Bahman Rahmatinejad<sup>1\*</sup>, Farzin Azimpour Shishevan<sup>2</sup>, Hadi Ghasemi Zavaragh<sup>3</sup>

<sup>1,2,3</sup>Department of Mechanical Engineering, Technical and Vocational University (TVU), Tehran, Iran.

### ARTICLE INFO

#### Article Type:

Original Research

**Received:** 02.20.2025

**Revised:** 04.11.2025

**Accepted:** 11.04.2025

#### Keyword:

CuO

Nano-fluid

Nanoparticles

Thermal Conductivity

Thermo-physical Properties

#### \*Corresponding Author:

Bahman Rahmatinejad

**Email:**

[brahmati@tvu.ac.ir](mailto:brahmati@tvu.ac.ir)

### ABSTRACT

This study experimentally examined the thermo-physical properties and thermal performance of CuO nanoparticles in water-based fluids and ethylene glycol. Four concentrations of nanofluids (1-4 volume percent) were prepared in the base fluids using an electric mixer, magnetic stirring, and ultrasonic oscillation, with a surfactant added to enhance stability. To measure the thermo-physical properties, the thermal conductivity was assessed. The findings demonstrated that adding 1% by weight of sodium dodecyl sulfate (SDS) to the CuO-water mixture stabilized the nanofluid for 20 days, resulting in a zeta potential of 37.7 mV, indicating good stability. Additionally, as the volume fraction of nanoparticles increased in the base fluid, there was an increase in thermal conductivity, density, steam pressure, and heating curve slope, while surface tension decreased. Moreover, with higher temperatures, the thermal conductivity and specific heat of water increased, whereas the density, viscosity, and specific heat of the nanofluid decreased with varying volume fractions. Such insights contribute to the broader understanding of nanofluid behavior, laying the groundwork for their application in enhanced thermal management systems.



## Introduction

For over a century, scientists and engineers have worked diligently to improve the thermal conductivity of traditional fluids, which is inherently low. This effort began with the dispersion of solid particles in fluids, initially using millimeter- and micrometer-sized particles, and has evolved to include solid nanoparticles. Today, nanofluids present a promising alternative to standard fluids like water and oil [1]. The introduction of nanoparticles significantly enhances the heat transfer properties of these nanofluids, leading to increased interest from researchers due to their unique characteristics and potential for improved thermal performance [2;3].

Numerous studies have investigated the factors influencing the heat transfer capabilities of CuO nanofluids. In 1995, Choi [2] was the first to demonstrate in a laboratory setting that combining solid metal and non-metallic nanoparticles with a base fluid could markedly enhance its thermal conductivity, coining the term "nanofluid" for the resulting suspension. Following Choi's work, many researchers have concentrated on improving the thermal properties of nanofluids [4]. Several key studies include. Das et al. (2007) explored the thermal behavior of water mixed with copper oxide and aluminum oxide nanofluids at varying temperatures, concluding that higher temperatures lead to increased thermal conductivity [5]. Mostafizur et al. (2014) examined the viscosity of  $\text{Al}_2\text{O}_3$  nanofluid as temperature changed, finding that rising temperatures enhance the Brownian motion of nanoparticles and reduce liquid adhesion, thereby lowering viscosity [6]. Khodaei (2020) investigated a mechanochemical reaction in a non-stoichiometric  $\text{Fe}_2\text{O}_3$ -Al system (a mixture of  $\text{Fe}_2\text{O}_3$ , Al, and Fe powders) to create a  $\text{Fe}_3\text{Al}$ -30 vol.%  $\text{Al}_2\text{O}_3$  nanocomposite. X-ray diffractometry (XRD) and transmission electron microscopy (TEM) were used to monitor the reaction progress. While XRD showed no evidence of the  $\text{Al}_2\text{O}_3$  phase, TEM confirmed its crystalline structure. The higher mass absorption coefficient of the  $\text{Fe}_3\text{Al}$  matrix reduced the diffraction intensity of the lower mass absorption coefficient components, like  $\text{Al}_2\text{O}_3$ . High-temperature treatment resulted in crystallite growth and reduced lattice strain, allowing for the detection of  $\text{Al}_2\text{O}_3$  by XRD [7]. Ni et al. (2017) studied the impact of an  $\text{Al}_2\text{O}_3$  coating on nickel, finding that the coated material exhibited greater stiffness and abrasion resistance compared to pure nickel [8]. Kračun et al. (2017) investigated the influence of  $\text{Al}_2\text{O}_3$  nanoparticle size on stainless steels, adding three volume fractions (0.5, 1, and 2.5) during conventional casting. Their results indicated that both particle size and concentration affected distribution [9]. Pugalenti et al. (2019) examined the reinforcing effects of SiC and  $\text{Al}_2\text{O}_3$  on aluminum composites, producing four samples via casting and demonstrating that the reinforcement materials enhanced tensile strength, resistance, and hardness [10]. Rahmatinejad et al. (2022) conducted an experimental evaluation of heat transfer in the MF 285 tractor radiator using a nanofluid based on water. Their findings

revealed that over 30% of the engine's heat energy is transferred by the cooling system. They identified two methods to improve heat transfer in automotive engines: optimizing radiator geometry and utilizing fluids with superior thermal properties. This research specifically examined the enhancement of radiator thermal performance by employing nanofluids in a laboratory model, exploring the effects of nanoparticle volume fraction and cooling flow rate on the heat transfer rate and coefficient [11]. Ajeeb et al. (2023) investigated the heat transfer performance of  $\text{Al}_2\text{O}_3$  nanofluids in a compact plate heat exchanger (PHE). This study experimentally assessed the performance of a gasketed PHE using  $\text{Al}_2\text{O}_3$  nanofluids at various low concentrations (0.01, 0.05, 0.10, 0.15, and 0.20 vol%) mixed with distilled water (DW) and ethylene glycol (EG) at two concentrations (15% and 30% EG) across several flow rates (0.03–0.093 l/s). Results indicated that heat transfer improved with increasing nanoparticle concentration, peaking at a 27% enhancement for the 0.2 vol% DW-based  $\text{Al}_2\text{O}_3$  nanofluid while experiencing an 8% increase in pressure drop. This enhancement was lower for higher percentages of EG, with a 19.1% increase for the 0.2 vol% in 30% EG nanofluid. Additionally, the energy efficiency factor rose with the addition of  $\text{Al}_2\text{O}_3$  nanoparticles and increased flow rates, reaching a maximum of 1.3 at the highest particle concentrations [12]. Rahmatinejad et al. (2021) examined the thermo-physical properties and thermal performance of  $\text{Al}_2\text{O}_3$  and CuO nanoparticles in water and ethylene glycol-based fluids. Their research indicated that increasing nanoparticle volume fraction, elevating temperature, and reducing nanoparticle diameter contributed to a higher thermal conductivity coefficient. They also found that the density of the fluid increased with nanoparticle volume fraction, noting that CuO-water nanofluid exhibited a higher density than the  $\text{Al}_2\text{O}_3$ -water mixture at equivalent fractions. The superior thermal properties of the base fluid enhanced the nanofluid's thermal conductivity [13]. Wanatasanappan et al. (2020) focused on the thermophysical properties of  $\text{Al}_2\text{O}_3$ -CuO hybrid nanofluids at various nanoparticle mixture ratios. They prepared a stable suspension with four distinct mixture ratios of 20:80, 40:60, 50:50, and 60:40 at a volume concentration of 1.0%. Thermal conductivity and viscosity were measured within a temperature range of 30°C to 70°C, revealing the highest thermal conductivity for the 60:40 ratio, with a maximum enhancement of 12.33% compared to the base fluid. Furthermore, viscosity decreased with rising temperature. Zeta potential analysis indicated that the hybrid sample with a 50:50 ratio exhibited moderate dispersion stability. A new correlation was proposed to predict the thermal conductivity of  $\text{Al}_2\text{O}_3$ -CuO hybrid nanofluids with an accuracy of 95%, and experiments demonstrated that the hybrid nanofluid performed significantly better thermally than the base fluid [14]. In another study, Rahmatinejad (2022) experimentally analyzed the thermo-physical properties and thermal performance of  $\text{Al}_2\text{O}_3$  nanoparticles in water-based fluid and ethylene glycol within a temperature range of 20°C to 50°C. Results indicated that adding 1% by weight of

sodium dodecyl benzene sulfonate (SDBS) stabilized the  $\text{Al}_2\text{O}_3 + \text{H}_2\text{O}$  nanofluid for 22 days, achieving a zeta potential of 37.7 mV, which indicated good stability. The study showed that increasing nanoparticle volume fraction in the base fluid raised thermal conductivity, density, vapor pressure, and heating curve slope, while reducing surface tension. With rising temperature, thermal conductivity and specific heat of water increased, whereas the density, viscosity, and specific heat of the nanofluid decreased with different volume fractions. Additionally, increasing nanoparticle diameter led to decreased thermal conductivity and increased surface tension of the nanofluid [15]. The growing use of nanofluids, known for their advanced thermal conductivity properties, across various industries necessitates a thorough understanding of their thermo-physical characteristics. Despite the limited comprehensive studies in this area and the inadequacy of classical models to precisely determine the thermal conductivity coefficients of nanofluids which have often yielded conflicting results this research aims to fill that gap. It involved laboratory determinations of these properties, which were then compared with established sources to evaluate the accuracy of the findings. Applications for nanofluids include heat exchangers, oscillating heat pipes, chillers, solar water heating systems, automotive engine cooling, electronic component cooling, and nuclear reactor cooling. This study primarily investigates the thermo-physical properties and thermal performance of CuO nanoparticles in water and ethylene glycol at various temperatures and volume fractions.

## Materials and methods

### *Synthesis of CuO Nanoparticles*

Recent methods for preparing nanocrystalline CuO include the sonochemical method [16], sol-gel technique [17], one-step solid-state reaction at room temperature [18], electrochemical method [19], thermal decomposition of precursors [20], and co-implantation of metal and oxygen ions [21]. All reagents used in these experiments were of analytical purity. The preparation process is illustrated in Figure 1.

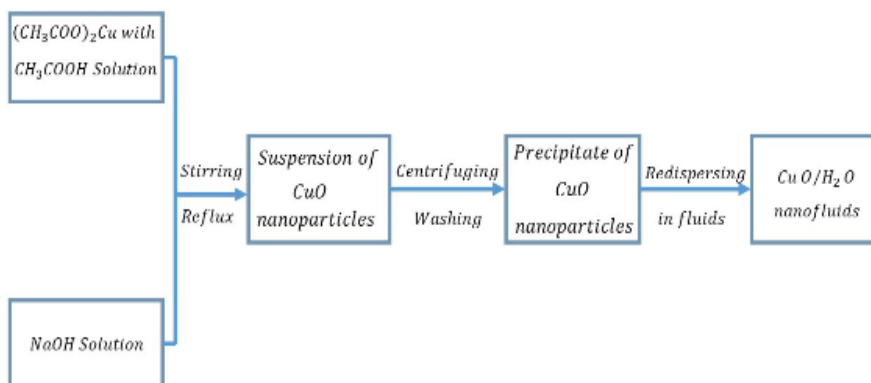
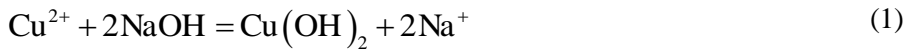


**Figure 1. Preparation process of CuO aqueous nanofluids**

The synthesis involves the following chemical reactions in solution:




An aqueous solution of copper acetate (0.02 mol) is prepared in a round-bottom flask. To this solution, 1 ml of glacial acetic acid is added and heated to 100°C with constant stirring. Approximately 0.4 g of NaOH is then added until the pH reaches 6-7, resulting in the immediate formation of a significant amount of black precipitate. The mixture is centrifuged and washed 3-4 times with deionized water. The resulting precipitate is dried in a hot-air oven for 24 hours, filtered using Whatman filter paper, and then ground into powder with a mortar for characterization and experimental analysis.

**Table 1. The elemental analysis of CuO nanoparticles.**

Elements (ppm)											
Ba	Cd	Co	Zn	Sr	Ca	K	p	Mg	Fe	Pb	Mn
0.75	2.5	6.4	195	2.3	400	300	300	75	87	90	3.5

**Table 2. Specifications of surfactants.**

sulfonate	Molecular formula	Formula structure	Molecular Weight (g/mol)	Density (g/cm <sup>3</sup> )
sodium dodecyl sulfate [22]	$\text{NaC}_{12}\text{H}_{25}\text{SO}_4$		288.372	1.01

Transmission electron microscopy (TEM) and scanning electron microscopy (SEM) images were obtained to analyze the structure and morphology of the

nanoparticles. TEM images were captured using a H9500 transmission electron microscope, while SEM images were taken with a HITACHI Su3500 scanning electron microscope (Fig. 2).

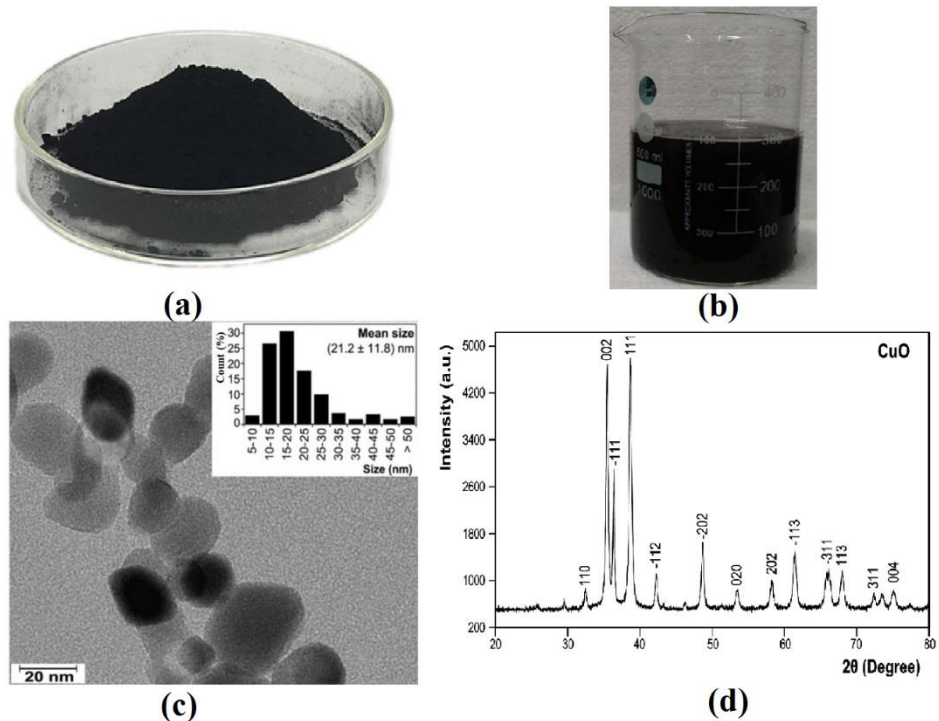


**Figure 2.** (a) CuO Nanoparticles, (b) CuO Nanofluids (c) TEM image of CuO nanoparticles with the histogram, (d) X-Ray diffraction (XRD) pattern of the CuO

Dynamic Light Scattering (DLS) and X-ray Diffraction (XRD) were employed to measure the nanoparticle diameter. In the DLS method, a laser beam is directed into the suspension, and the scattering of the laser light is detected by an optical sensor. Particles of different sizes scatter light differently: larger particles scatter light at smaller angles, while smaller particles scatter light at wider angles. This scattering creates a pattern of light and dark spots on the detector, which changes over time as the particles move. The DLS software analyzes these changes to determine the particle size distribution, with larger particles moving more slowly than smaller ones. The relationship between particle size and Brownian motion speed is described by the Stokes-Einstein equation:

$$d_H = \frac{KT}{3\pi\eta d} \quad (3)$$

dH: Hydrodynamic Diameter of Particle, K: Boltzmann constant,  $\eta$ : solvent viscosity that depends on temperature and is not related to system density and pressure. T: Absolute temperature and d: Influence coefficient [23].

Figure 3 shows that all diffraction peaks correspond to cupric oxide (CuO), confirming that the products obtained are solely CuO. The characteristic peak of CuO appears at an angle of  $38.44^\circ$ , consistent with its characterization limits of  $35.7^\circ$  to  $38.5^\circ$  [24]. The XRD patterns indicate the formation of a single phase with high purity and crystallinity, as evidenced by the narrow and intense peaks [25]. The intensities and positions of these peaks align well with reported values (JCPDS file No. 05-661).

In the XRD diffraction method, to determine the size of the nanoparticles, the processing and analysis of the X-ray return from the sample surface is examined. In the XRD method, the particle size is calculated from Equation 4.

$$D = \frac{0.93 \lambda}{B \cos \theta_B} \quad (4)$$

K: Shape coefficient (for spherical nanoparticles  $K = 0.93$ ),  $\lambda$ : X-ray wavelength, D: Particle diameter, B: Maximum peak width at half height,  $\theta$ : The scattering angle for which the maximum peak is formed.

The thermophysical properties of CuO nanoparticles are shown in Table 3.

**Table 3. Thermophysical properties of CuO nanoparticles**

Material	CuO
Diameter	<20 nm
Purity	99%
Density	6510 $kg / m^3$
Specific heat capacity	540 J/kgK
Thermal conductivity	33 W/mK

The thermophysical properties of CuO nanoparticles are summarized in Table 3. The Energy Dispersive Spectroscopy (EDS) spectra of CuO thin film samples (Figure 3) clearly show peaks corresponding only to Cu and O elements. The observed atomic ratio of 2:1 between Cu and O suggests the presence of  $Cu_2O$  in these films; however, the XRD results indicate that the films predominantly consist of CuO. The XRD patterns also reveal peaks corresponding to metallic Cu from the Cu substrate, as the films are

thin. Thus, the excess Cu observed in the EDS results arises from the substrate, with no peaks indicating other elements beyond Cu and O.

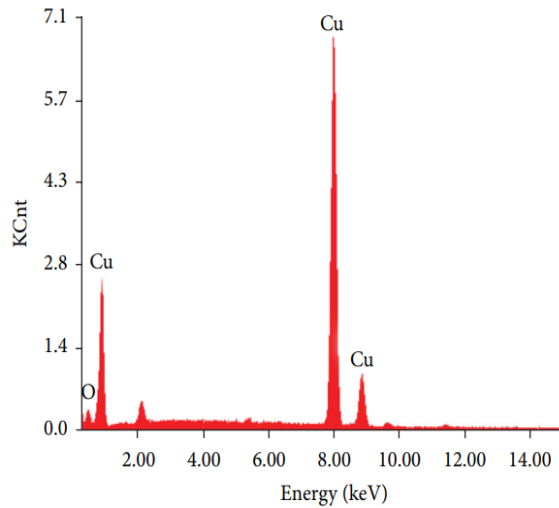


**Figure 3.** EDS spectra of CuO thin films prepared at substrate temperature of 30°C

To prepare the nanofluid, an electric mixer capable of adjusting speeds from 200 to 3000 rpm was employed, followed by a magnetic shaker operating at 100 to 2000 rpm with a heating power of 400 W. To ensure solution stability suitable for engineering applications, 1% by weight of surfactant (sodium dodecyl sulfate) was added. The properties of the surfactants are detailed in Table 3.

The mass of nanoparticles ( $m_p$ ) and the mass of the base fluid ( $m_f$ ) were measured accurately (0.01 g). Equation 5 can be used to estimate the weight percentage [26].

$$\phi = \left( \frac{m_p}{m_p + m_f} \right) \times 100 \quad (5)$$

If we show the density of nanoparticles ( $\rho_{np}$ ) and the density of the base fluid with ( $\rho_{bf}$ ), we can estimate the volume concentration of nanoparticles in the base fluid from equation 6 [27].

$$\% (\varphi) = \left[ \frac{\frac{W_{np}}{\rho_{np}}}{\frac{W_{np}}{\rho_{np}} + \frac{W_{bf}}{\rho_{bf}}} \right] \times 100 \quad (6)$$

In equation 6 the bf index is for the base fluid and np for the nanoparticles.

### ***Determination of thermophysical properties of nanofluid***

#### ***Determination of Thermal Conductivity Coefficient Using Maxwell- Garnett model and Transient Hot Wire Method***

The thermal conductivity coefficient was calculated using the Maxwell-Garnett model, which aligns well with the experimental data [28]. The relationship is expressed as:

$$\frac{K_{nf}}{K_f} = \frac{(K_p + 2K_f) - 2\varphi(K_f - K_p)}{(K_p + 2K_f) + \varphi(K_f - K_p)} \quad (7)$$

To validate the results obtained from the Maxwell-Garnett model, the thermal conductivity coefficient was also recalculated using the transient hot wire method. This method is commonly employed for the experimental measurement of thermal conductivity in liquids, both statically and with a linear source. In this research, the transient hot wire method outlined in Rahmatinejad's study was utilized to determine the thermal conductivity coefficient [11]. The transient hot wire method allows us to measure k quickly and accurately, while also reducing the unwanted effects of thermal conductivity. The accuracy of the Hot Wire sensor was calibrated by measuring the thermal conductivity of pure water. The uncertainty of the measured values was estimated to be  $\pm 1\%$ .

#### ***Density, specific heat capacity and dynamic viscosity***

The density, specific heat capacity, and dynamic viscosity of the prepared nanofluid can be calculated using the formulas provided in this study. The density of the nanofluid can be determined using the law of mixtures based on the Pak and Chow relation [29]:

$$\rho_{nf} = (1 - \phi_p) \rho_b + \phi_p \rho_p \quad (8)$$

$\rho_{nf}$  is the density of the nano-fluid,  $V_b$  is the volume of the base fluid and  $V_p$  is the volume of the nanoparticles. In this regard,  $\phi$  the volume fraction of nanoparticles,  $\rho$  density, and index p represent nanoparticles and b represents the base fluid. Most researchers use Equation 9 to determine specific heat capacity [30].

$$C_{p,nf} = \frac{(1-\phi_p)(\rho C_p)_b + \phi_p(\rho C_p)_p}{(1-\phi_p)\rho_b + \phi_p\rho_p} \quad (9)$$

$C_{p,nf}$  is the specific heat constant pressure of the nano-fluid, index P for nanoparticles and index b for the base fluid. Various theoretical models have been proposed to calculate the viscosity of nano-fluids, among which the Brinkman model was used in this study [31].

$$\frac{\mu_{nf}}{\mu_f} = (1-\phi)^{2.5} \quad (10)$$

$\phi$  is the volume fraction of nanoparticles,  $\mu_f$  the dynamic viscosity of the base fluid, and  $\mu_{nf}$  the dynamic viscosity of the nano-fluid. In order to evaluate the results of Equation (14), the viscosity of the nano-fluid was calculated experimentally by the ASTM D445-06 Ostwald viscometer. The accuracy of the device is  $\pm 0.07\%$  and a recording discrimination of 0.1 s according. The DA130N digital portable density meter of KEM company of Japan was used to measure the density and the KRUSS K11 Tensiometer was used to measure the surface tension.

The uncertainty in viscosity measurement was calculated based on the accuracy of the viscometer ( $\pm 1\%$ ), the precision of the electronic balance ( $\pm 0.0004$  g), and the thermal circulator bath ( $\pm 0.005$  °C). The overall uncertainty was determined using the following equation [32]:

$$U_{\text{Dynamic viscosity}} = \pm \sqrt{\left(\frac{\Delta\mu}{\mu}\right)^2 + \left(\frac{\Delta w}{w}\right)^2 + \left(\frac{\Delta T}{T}\right)^2} \quad (11)$$

Using this equation, the maximum measurement uncertainty was found to be  $\pm 4.6\%$ .

## Result and discussion

### *Investigation of nanoparticle sedimentation in nano-fluids*

One key factor influencing the stability of nanofluids is the formation of clusters or the accumulation of particles, which can lead to sedimentation. To examine the settling time, a mixture of CuO nanofluid and water was prepared. To enhance the stability of this solution for engineering applications, 1% by weight of sodium dodecyl sulfate (SDS) was added as a surfactant. According to stability theory, a high absolute value of zeta potential indicates increased electrostatic repulsion between particles, resulting in better suspension stability. Particles with a high surface charge are less likely to form clusters. Many researchers, including [33], have noted that colloidal solutions remain stable at zeta potentials exceeding 30 mV. A Zeta potential analyzer (ZETA-Check model from Particle Metrix, Germany) was used to measure the zeta potential, utilizing 2 wt% CuO nanoparticles with a diameter of 20 nm. The experiment was conducted at 25 °C, with a pressure of one atmosphere and humidity at 38%. The highest measured zeta potential for the CuO + H<sub>2</sub>O nanofluid was 37.7 mV, indicating excellent stability and dispersion.

### *Thermal Conductivity Coefficient*

The thermal conductivity of CuO nanofluid was tested at volume percentages of 1%, 2%, 3%, and 4%, and the results were evaluated using the Maxwell-Garnett model. Both experimental data and theoretical predictions show that the thermal conductivity coefficient increases with the volume fraction (Fig. 4).

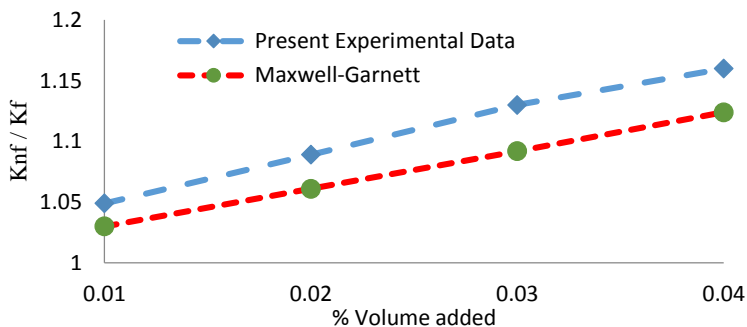


**Figure 4.** Display changes in theoretical thermal conductivity coefficient by changing the volume deduction (CuO + water)

### *Investigating the Effect of Nanoparticle Diameter on Nanofluid Thermal Conductivity*

The thermal conductivity coefficient of CuO nanoparticles suspended in water was examined at volume fractions of 1% to 4% for nanoparticles with diameters of 8 nm and 25 nm, as shown in Figure 5.

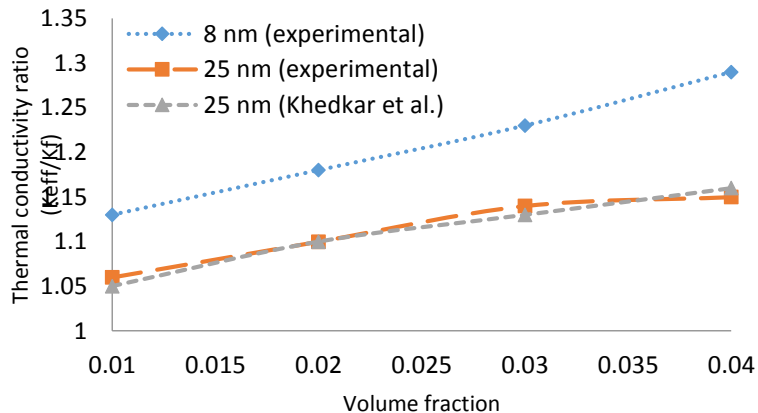


**Figure 5.** The effect of nanoparticle size in different volume deduction on the effective thermal conductivity coefficient of CuO + Water

The effect of nanoparticle size on the thermal conductivity of nanofluids is a complex phenomenon influenced by several factors, including the surface-to-volume ratio and inter-particle distance. The results indicate that smaller nanoparticle diameters lead to higher thermal conductivity coefficients. This is attributed to the increased surface-to-volume ratio, which enhances thermal contact with the fluid. As the diameter of nanoparticles decreases from 25 nm to 8 nm, the surface-to-volume ratio increases significantly. This higher ratio generally leads to enhanced thermal interfaces that can facilitate heat transfer, as a greater proportion of the material is exposed to the surrounding fluid. As the size of the nanoparticles decreases and their concentration increases, inter-particle distances can change. Closer proximity between nanoparticles can enhance conductive pathways through particle networks, positively impacting thermal conductivity. When nanoparticles are closer together, heat transfer through conduction between them can become more effective, which may offset any potential decrease in thermal conductivity due to size alone. The interaction of smaller nanoparticles with the base fluid can affect the overall viscoelastic properties of the nanofluid, thereby influencing the effective thermal conductivity. Specifically, reducing the nanoparticle diameter from 25 nm to 8 nm resulted in a thermal conductivity increase of approximately 12%.

### *Investigating the modifications within the Thermal Conductivity Coefficient of Nanofluids with the Volumetric percent of Nanoparticles*

The thermal conductivity of CuO + water was assessed at volume percentages ranging from 1% to 5%. The results, illustrated in Figure 6, demonstrate that the effect of increasing volume fraction can be either linear or nonlinear, depending on the system. The thermal conductivity of nanofluids is influenced by both the thermal conductivity of the base fluid and that of the nanoparticles. For instance, increasing the volume fraction of CuO from 1% to 5% resulted in an approximate 12% increase in thermal conductivity, consistent with findings from [34].

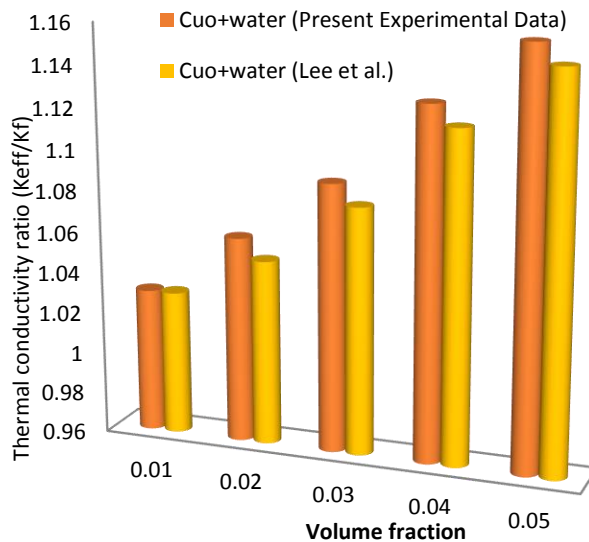


**Figure 6.** Investigation of changes in thermal conductivity coefficient of nanofluid CuO + Water with volumetric percentage of nanoparticles

### *Determination of nanofluid density and specific heat*

Density measurements were conducted using a DA130N device. The results reveal that the density of the nanofluids is significantly higher than that of water-based fluids, and it increases with the volume fraction of nanoparticles. Specifically, a 9% increase in density was observed when the volume fraction of CuO increased from 1% to 4%. These findings were compared with literature sources [29; 30; 35] (Fig. 7).

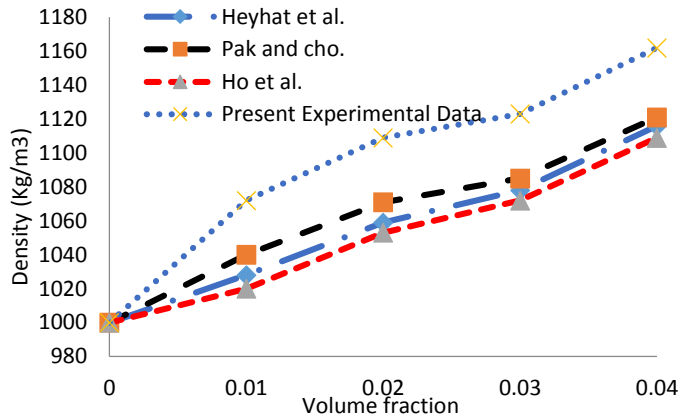


**Figure 7. Nano-fluid density CuO + Water with volumetric percentages 1 to 4**

As temperature increases, fluids typically expand, leading to changes in density. However, not all fluids expand at the same rate. The impact of temperature on nanofluid density was further investigated, revealing that density decreases with rising temperature. The decrease in the density of nanofluids with increasing temperature is primarily attributed to thermal expansion of the base fluid, but there are other factors at play as well. Other factors—such as nanoparticle interactions, structural changes, and interfacial effects—can also contribute to a lesser extent. The interplay of these factors can become quite complex, especially in concentrated nanofluids or under varied thermal conditions. Prasher and colleagues found that increasing the density of nanoparticles in the nanofluid reduces the heat transfer through Brownian motion due to increased inertia and decreased mobility of the nanoparticles [36].

Specific heat was measured using a KD2-Pro device across a temperature range of 20 to 100 °C. During this range, the specific heat of water increased by 0.9%. In contrast, for volume fractions of 1% to 4%, specific heat decreased by 3%, 5.7%, 8.5%, and 11.2%, respectively (Fig. 8).

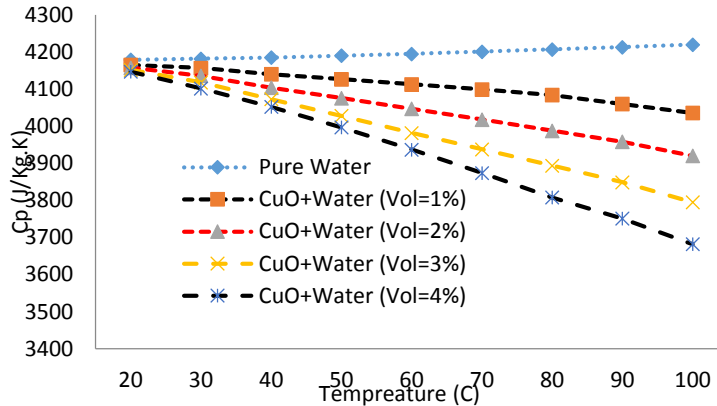


**Figure 8. Specific heat changes of water-based fluid and nano-fluid CuO + H<sub>2</sub>O with respect to temperature**

### *Investigation of dynamic viscosity of nanofluids*

The viscosity of CuO nanofluid was measured using nanoparticles with a diameter of 20 nm. Temperature significantly impacts viscosity; as temperature increases, the viscosity of gases rises, while the viscosity of liquids decreases (Fig. 9). This phenomenon can be explained by analyzing the factors affecting viscosity. The results were compared with data from sources [26] and [37]. At 30 °C and a volume fraction of 2%, the viscosity increased by 53% compared to the base fluid.

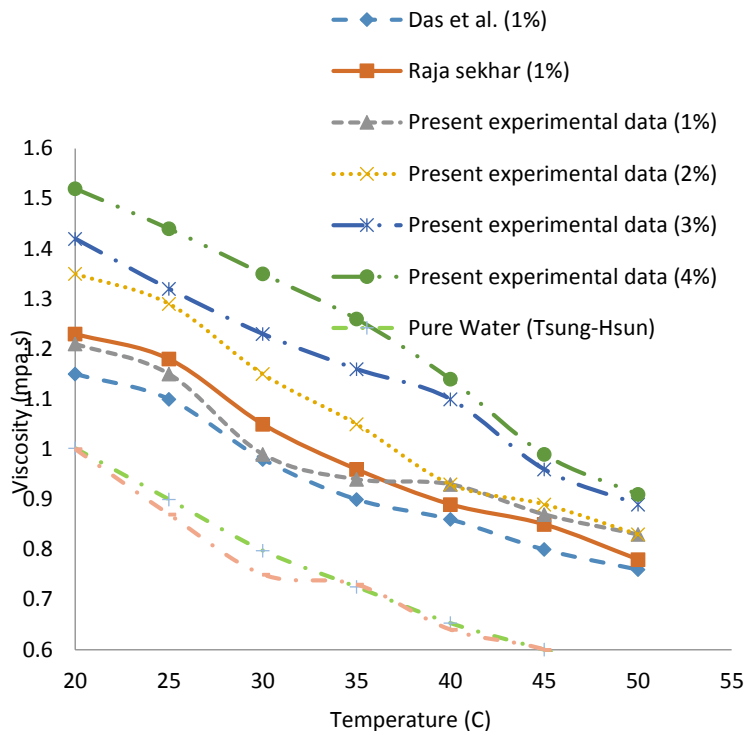


**Figure 9. Viscosity changes of pure water and nanofluid CuO+water with temperature changes**

The decrease in the viscosity of nanofluids with increasing temperature is influenced by several factors, primarily the reduction in intermolecular forces and the effects of Brownian motion. As temperature rises, the thermal energy of the fluid molecules increases. This higher energy level means that the molecules move more vigorously, which reduces the strength of intermolecular forces (like van der Waals forces) that contribute to viscosity. With stronger thermal motion, the cohesive forces between the fluid molecules weaken, allowing them to flow more easily past one another, thereby reducing viscosity. At higher temperatures, the increased kinetic energy enhances Brownian motion, leading to better dispersion of nanoparticles within the fluid. This improved distribution can reduce localized concentrations of nanoparticles that might otherwise increase viscosity. The motion of nanoparticles can disrupt any structured regions in the fluid that may develop at lower temperatures, further contributing to a decrease in viscosity. The base fluid (e.g., water, oil) itself typically experiences a decrease in viscosity with increasing temperature. This temperature dependency can play a significant role in the overall viscosity of the nanofluid.

A decrease in nanoparticle diameter can significantly affect the viscosity of nanofluids. Smaller nanoparticles have a higher surface-to-volume ratio, which increases the area available for interaction with the fluid. This greater surface area can enhance the effective viscosity of the fluid due to the increased interactions between the nanoparticles and the base fluid. Smaller nanoparticles experience enhanced Brownian motion at given temperatures due to their reduced mass. This increased movement can lead to better dispersion within the fluid, potentially reducing the effective viscosity by preventing clustering or aggregation. Better dispersion can improve the heat transfer characteristics of the fluid, indirectly affecting viscosity through altered thermal gradients caused by temperature variations. As nanoparticle size decreases, the distance between particles may decrease if the concentration of nanoparticles remains the same. This can alter how particles interact with each other and the base fluid, impacting the overall viscosity.

### *The effect of temperature in different volume percentages on the thermal conductivity Coefficient of nanofluids*

The 20 nm copper oxide nanofluid was tested in water at volume fractions of up to 2% and temperatures ranging from 20 to 50 °C. The thermal conductivity coefficient was accurately measured and recorded, with results displayed in Figure 10.

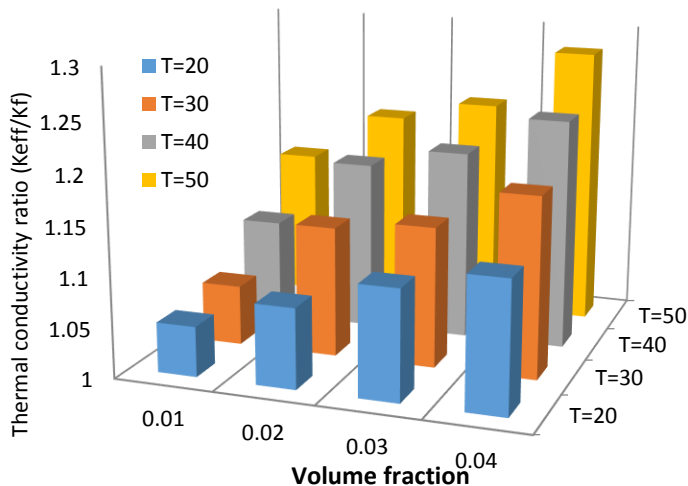


**Figure 10.** Changes in the ratio of thermal conductivity coefficient to volume deduction for nanofluid copper oxide in water at different temperatures

To verify the accuracy of the measurements obtained for a 0.01 volume fraction at temperatures between 20 and 50 °C, a comparison was made with data from source [26]. The results indicate that at lower volume fractions, variations in temperature have

minimal impact on the thermal conductivity coefficient, resulting in only slight differences. However, as the volume fraction increases, the effect of temperature on thermal conductivity becomes more pronounced. An increase in volume fraction also leads to a greater number of particles in the base fluid, which, combined with the elevated temperature, enhances molecular collisions and Brownian motion. For example, at a volume fraction of 2%, the thermal conductivity increased by approximately 11% when the temperature rose from 20 to 50 °C.

### ***Comparison CuO thermal conductivity coefficient with water and ethylene glycol base fluids***

The effect of copper oxide nanoparticle addition on thermal conductivity was studied in two common base fluids, water and ethylene glycol, at varying volume fractions. Results show that the more thermally conductive the fluid, the greater the impact of nanoparticles on its thermal conductivity coefficient. For instance, at 30 °C, the thermal conductivity coefficient of ethylene glycol is 0.28, while for water, it is 0.62. When comparing mixtures of both base fluids with CuO, the thermal conductivity coefficient of the mixture with ethylene glycol is lower than that of the mixture with water (Fig. 11).

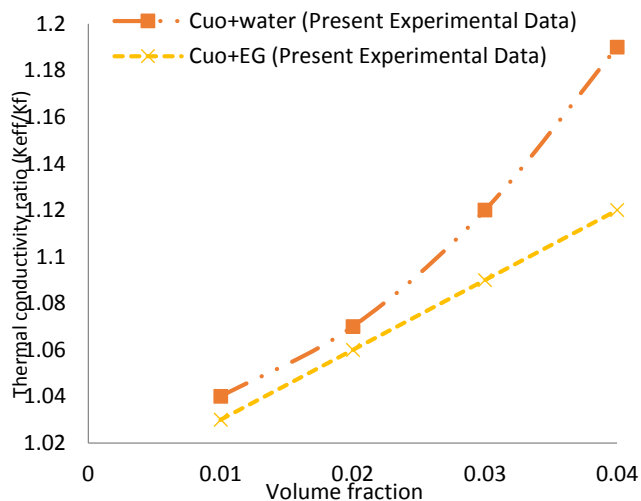


**Figure 11. Comparison CuO thermal conductivity coefficient with water and ethylene glycol base fluids**

### ***Surface tension check***

Surface tension was measured using the KRUSS K11 tensiometer. The concentration, temperature, and size of the nanoparticles affect surface tension. As

concentration and temperature increase, surface tension decreases due to enhanced molecular motion, which reduces intermolecular forces. However, in CuO nanofluids, surface tension remains relatively constant despite increases in volume concentration. This suggests that particle volume concentration does not significantly affect the surface tension of nanofluids. A decrease in nanoparticle diameter can affect the surface tension of nanofluids. Smaller nanoparticles increase the surface area-to-volume ratio, which enhances their interaction with the base fluid and can lead to more significant modifications to the fluid's properties. This increased surface area may result in a greater density of nanoparticles at the fluid's interface, which can alter the surface structure and potentially reduce surface tension. Additionally, the ability of smaller nanoparticles to better disperse and stabilize within the fluid can contribute to changes in interfacial properties, influencing overall surface tension. Figure 12 illustrates the relationship between surface tension and volume concentration.

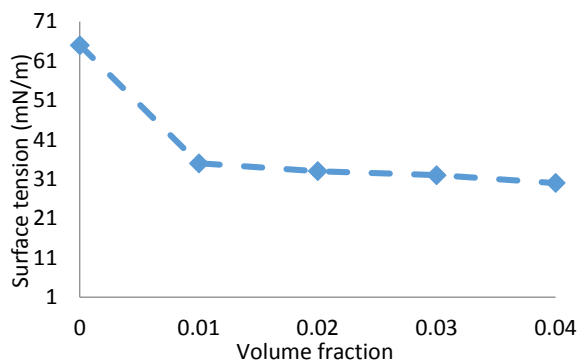


**Figure 12.** Surface tension measurement of the CuO nanofluids as a function of the volume concentration

## Conclusion

In this study, CuO nanoparticles were blended with water and ethylene glycol at volume fractions of 1% to 4% using an electric mixer. The stability of nanofluids remains a complex challenge, necessitating the addition of surfactants to improve their suitability for practical applications. To address this, SDS was added to the CuO solution, resulting in stable nanofluids for up to 20 days. Increasing volume fraction, temperature, and decreasing nanoparticle diameter enhance the thermal conductivity coefficient. Furthermore, as the volume fraction of nanoparticles in the base fluid increases, the overall density also rises. The results indicate a significant reduction in density with increasing temperature. In conclusion, the analysis of thermophysical properties of CuO nanoparticles in water and ethylene glycol-based fluids reveals their promising potential for various industrial applications, particularly in high-temperature environments. The stability of CuO nanofluids at elevated temperatures

enhances their suitability for use in heat transfer systems, cooling applications, and various thermal management processes. Thus, with the appropriate development and implementation strategies, CuO nanofluids hold great promise for advancing thermal management solutions in real industrial systems.

## References

- [1] Asadi Borojeni, B., & Khosravi Farsani, A. (2024). Numerical Simulation of Laminar Nanofluids Flow in a Curved Duct with a Square Cross-section. *Karafan Journal*, 21(1), 411-433. <http://doi.org/10.48301/kssa.2024.427698.2775>
- [2] Choi, S. U., & Eastman, J. A. (1995). Enhancing thermal conductivity of fluids with nanoparticles.
- [3] Mousavi, S. V. (2024). Numerical Study of Flow and Heat Transfer of Magnetic Nanofluid in a Tee Channel in the Presence of Variable Magnetic Field. *Karafan Journal*, 21(1), 453-481. <http://doi.org/10.48301/kssa.2024.413755.2683>
- [4] Gonçalves, I., Souza, R., Coutinho, G., Miranda, J., Moita, A., Pereira, J. E., Moreira, A., & Lima, R. (2021). Thermal conductivity of nanofluids: A review on prediction models, controversies and challenges. *Applied Sciences*, 11(6), 2525. <https://doi.org/10.3390/app11062525>
- [5] Das, S. K., Choi, S. U., Yu, W., & Pradeep, T. (2007). *Nanofluids: science and technology*. John Wiley & Sons.
- [6] Mostafizur, R., Aziz, A. A., Saidur, R., Bhuiyan, M., & Mahbulul, I. (2014). Effect of temperature and volume fraction on rheology of methanol based nanofluids. *International Journal of Heat and Mass Transfer*, 77, 765-769. <https://doi.org/10.1016/j.ijheatmasstransfer.2014.05.055>
- [7] Khodaei, M. (2020). Characterization of Al<sub>2</sub>O<sub>3</sub> in Fe<sub>3</sub>Al-30 vol.% Al<sub>2</sub>O<sub>3</sub> nanocomposite powder synthesized by mechanochemical process. *Journal of Nanostructures*, 10(3), 456-462. <https://doi.org/10.22052/JNS.2020.03.003>
- [8] Ni, K. P. N., & KOMPOZITIH, N. O. (2017). The effect of current types on the microstructure and corrosion properties of Ni/NanoAl<sub>2</sub>O<sub>3</sub> composite coatings. *Materiali in tehnologije*, 51(3), 403-411. <https://doi.org/10.17222/mit.2015.347>
- [9] NERJAVNEM, P. D. A. O. V. A. DISTRIBUTION OF Al<sub>2</sub>O<sub>3</sub> REINFORCEMENT PARTICLES IN AUSTENITIC STAINLESS STEEL DEPENDING ON THEIR SIZE AND CONCENTRATION. *matrix*, 6, 8. <https://doi.org/10.17222/mit.2017.042>
- [10] Pugalenth, P., Jayaraman, M., & Subburam, V. (2019). Study of the microstructures and mechanical properties of aluminium hybrid composites with. *Materiali in tehnologije*, 53(1), 49-55. <https://doi.org/10.17222/mit.2018.118>
- [11] Rahmatinejad, B. (2022). Investigating thermophysical properties and thermal performance of Al<sub>2</sub>O<sub>3</sub> nanoparticles in water and ethylene glycol based fluids. *Journal of Nanostructures*, 12(3), 642-659. <https://doi.org/10.22052/JNS.2022.03.018>

- [12] Ajeeb, W., da Silva, R. R. T., & Murshed, S. S. (2023). Experimental investigation of heat transfer performance of Al<sub>2</sub>O<sub>3</sub> nanofluids in a compact plate heat exchanger. *Applied Thermal Engineering*, 218, 119321. <https://doi.org/10.1016/j.applthermaleng.2022.119321>
- [13] Rahmatinejad, B., Abbasgholipour, M., & Alasti, B. M. (2021). Investigating thermo-physical properties and thermal performance of Al<sub>2</sub>O<sub>3</sub> and CuO nanoparticles in Water and Ethylene Glycol based fluids. *International Journal of Nano Dimension*, 12(3). <https://doi.org/10.22034/ijnd.2021.681560>
- [14] Wanatasanappan, V. V., Abdullah, M., & Gunnasegaran, P. (2020). Thermophysical properties of Al<sub>2</sub>O<sub>3</sub>-CuO hybrid nanofluid at different nanoparticle mixture ratio: An experimental approach. *Journal of Molecular Liquids*, 313, 113458. <https://doi.org/10.1016/j.molliq.2020.113458>
- [15] Rahmatinejad, B., Abbasgholipour, M., & Alasti, B. M. Experimental Evaluation of Heat Transfer of MF 285 Tractor Radiator, using Nano-fluid Water. *Journal of Agricultural Machinery*, 12(3), 281-299. <https://doi.org/10.22067/jam.2020.58870.0>
- [16] Yin, L., Wang, Y., Pang, G., Kolytyn, Y., & Gedanken, A. (2002). Sonochemical synthesis of cerium oxide nanoparticles—effect of additives and quantum size effect. *Journal of Colloid and Interface Science*, 246(1), 78-84. <https://doi.org/10.1006/jcis.2001.8047>
- [17] Eliseev, A. A., Lukashin, A. V., Vertegel, A. A., Heifets, L. I., Zhirov, A. I., & Tretyakov, Y. D. (2000). Complexes of Cu (II) with polyvinyl alcohol as precursors for the preparation of CuO/SiO<sub>2</sub> nanocomposites. *Materials Research Innovations*, 3(5), 308-312. <https://doi.org/10.1007/PL00010877>
- [18] Xu, J., Ji, W., Shen, Z., Tang, S., Ye, X., Jia, D., & Xin, X. (1999). Preparation and characterization of CuO nanocrystals. *Journal of Solid State Chemistry*, 147(2), 516-519. <https://doi.org/10.1006/jssc.1999.8409>
- [19] Borgohain, K., Singh, J. B., Rao, M. R., Shripathi, T., & Mahamuni, S. (2000). Quantum size effects in CuO nanoparticles. *Physical Review B*, 61(16), 11093. <https://doi.org/10.1103/PhysRevB.61.11093>
- [20] Yu, J., Xu, Z., Jia, D., & Chin, J. (1999). Decontamination Procedure of CEES on to the Surface of CuO NPs. *Funct. Mater. Instrum.*, 5, 267-273.
- [21] Nakao, S., Ikeyama, M., Mizota, T., Jin, P., Tazawa, M., Miyagawa, Y., Miyagawa, S., Wang, S., & Wang, L. (2000). Attempts of the formation of metal oxide nano-particles by co-implantation of metal and oxygen ions. REPORT-RESEARCH CENTER OF ION BEAM TECHNOLOGY HOSEI UNIVERSITY-SUPPLEMENT-, 153-158.
- [22] Hwang, Y., Lee, J.-K., Lee, J.-K., Jeong, Y.-M., Cheong, S.-i., Ahn, Y.-C., & Kim, S. H. (2008). Production and dispersion stability of nanoparticles in nanofluids. *Powder technology*, 186(2), 145-153. <https://doi.org/10.1016/j.powtec.2007.11.020>
- [23] Pecora, R. (2013). *Dynamic light scattering: applications of photon correlation spectroscopy*. Springer Science & Business Media.

- [24] Urquieta-González, E. A., Martins, L., Peguin, R., & Batista, M. (2002). Identification of extra-framework species on Fe/ZSM-5 and Cu/ZSM-5 catalysts typical microporous molecular sieves with zeolitic structure. *Materials Research*, 5, 321-327. <https://doi.org/10.1590/S1516-14392002000300017>
- [25] Jamil, Y., Ahmad, M. R., Hafeez, A., & Zia-ul-Haq, A. N. (2008). Microwave assisted synthesis of fine magnetic manganese ferrite particles using co-precipitation technique. *Pak. J. Agri. Sci*, 45(3), 59-64.
- [26] Das, S. K., Putra, N., Thiesen, P., & Roetzel, W. (2003). Temperature dependence of thermal conductivity enhancement for nanofluids. *J. Heat Transfer*, 125(4), 567-574. <https://doi.org/10.1115/1.1571080>
- [27] Leong, K. Y., Saidur, R., Kazi, S., & Mamun, A. (2010). Performance investigation of an automotive car radiator operated with nanofluid-based coolants (nanofluid as a coolant in a radiator). *Applied Thermal Engineering*, 30(17-18), 2685-2692. <https://doi.org/10.1016/j.applthermaleng.2010.07.019>
- [28] Mahmood, F. E., & Abdullah, F. Y. (2022). Modeling and analysis of millimeter-wave propagation in dusty environments. *TELKOMNIKA (Telecommunication Computing Electronics and Control)*, 20(4), 715-721. <http://doi.org/10.12928/telkomnika.v20i4.23245>
- [29] Pak, B. C., & Cho, Y. I. (1998). Hydrodynamic and heat transfer study of dispersed fluids with submicron metallic oxide particles. *Experimental Heat Transfer an International Journal*, 11(2), 151-170. <https://doi.org/10.1080/08916159808946559>
- [30] Ho, C., Liu, W., Chang, Y., & Lin, C. (2010). Natural convection heat transfer of alumina-water nanofluid in vertical square enclosures: An experimental study. *International Journal of Thermal Sciences*, 49(8), 1345-1353. <https://doi.org/10.1016/j.ijthermalsci.2010.02.013>
- [31] Brinkman, H. C. (1952). The viscosity of concentrated suspensions and solutions. *The Journal of chemical physics*, 20(4), 571-571. <https://doi.org/10.1063/1.1700493>
- [32] Teng, T.-P., Hung, Y.-H., Teng, T.-C., Mo, H.-E., & Hsu, H.-G. (2010). The effect of alumina/water nanofluid particle size on thermal conductivity. *Applied Thermal Engineering*, 30(14-15), 2213-2218. <https://doi.org/10.1016/j.applthermaleng.2010.05.036>
- [33] Wu, S., Zhu, D., Li, X., Li, H., & Lei, J. (2009). Thermal energy storage behavior of Al<sub>2</sub>O<sub>3</sub>-H<sub>2</sub>O nanofluids. *Thermochimica Acta*, 483(1-2), 73-77. <https://doi.org/10.1016/j.tca.2008.11.006>
- [34] Lee, S., Choi, S.-S., Li, S., and, & Eastman, J. (1999). Measuring thermal conductivity of fluids containing oxide nanoparticles. <https://doi.org/10.1115/1.2825978>
- [35] Heyhat, M., Kowsary, F., Rashidi, A., Esfehiani, S. A. V., & Amrollahi, A. (2012). Experimental investigation of turbulent flow and convective heat transfer characteristics of alumina water nanofluids in fully developed flow regime. *International*

- Communications in Heat and Mass Transfer, 39(8), 1272-1278.  
<https://doi.org/10.1016/j.icheatmasstransfer.2012.06.024>
- [36] Prasher, R., Bhattacharya, P., & Phelan, P. E. (2005). Thermal conductivity of nanoscale colloidal solutions (nanofluids). Physical review letters, 94(2), 025901.  
<https://doi.org/10.1103/PhysRevLett.94.025901>
- [37] Sekhar, Y. R., & Sharma, K. (2015). Study of viscosity and specific heat capacity characteristics of water-based Al<sub>2</sub>O<sub>3</sub> nanofluids at low particle concentrations. Journal of experimental Nanoscience, 10(2), 86-102.  
<https://doi.org/10.1080/17458080.2013.796595>